Author Accepted Manuscript version of the paper by Jie Yan et al.
in 12th International Conference on Renewable Power Generation - RPG (2023)
DOI: http://dx.doi.org/10.1049/icp.2023.2492

Impact of wind farm wake steering control on blade root load

Jie Yan[1*], Kaibo Wang[1], Hangyu Wang[1], Valentin Chabaud[2], Shukai He[1], Yongqian Liu[1]

[1]School of New Energy, North China Electric Power University, Beijing 102206, China

[2]SINTEF Energy Systems Department, SINTEF Energy Research AS, Sem Sælands veg 11, 7034 Norway

**yanjie@ncepu.edu.cn*

Keywords: WAKE STEERING CONTROL, WIND FARM SIMULATION, LOAD CALCULATION

Abstract

Yaw misalignment is known to affect blade root loads on wind turbines. Most of previous studies concentrate on yaw misalignment in the context of wake steering control, aiming at increasing the total output power of the wind farm. There, wake steering is compared with greedy control, in which yaw misalignment is considered to be 0. In reality, yaw misalignment also occurs in greedy control due to changes in wind direction arising from varying inflow conditions (e.g. turbulence). This paper aims at comparing these two sources of yaw misalignment —naturally changing wind direction versus active yaw in wake steering— in terms of blade root loads. To this end, SCADA data from a real wind farm is used to get yaw misalignment statistics in actual greedy control conditions. FAST.Farm is used to simulate three wind turbines arranged in series, to study maximum and damage-equivalent loads corresponding to in-plane and out-of-plane bending moments on the blades. The results show that compared with actual greedy control, wake steering control reduces the maximum load from the upstream wind turbine, but increases it from other wind turbines. Concerning the damage-equivalent loads from all wind turbines, the blade's in-plane moment is reduced, but the blade's out-of-plane moment is increased.

1 Introduction

With wind farms' up-scaling, wake effects have become a major factor restricting wind power generation [1]. Wake steering control of the wind farm significantly improves the overall output of the wind farm by mitigating the wake induced velocity deficit on downstream turbines; and has the potential to improve the benefit of wind farms [2]. Recently, relevant tests have been carried out in the actual wind farms [3][4] using wake steering for power maximization. However, wake steering changes the yaw angle distribution on upstream turbines and flow on downstream turbines, affecting structural loads as a side effect [5].

The effect of wake steering on structural loads has been analyzed in numerous numerical and experimental studies ([6][7][8], among others). Previous studies have shown that there is a complex relationship between blade root fatigue, ultimate load, and yaw misalignment [9]. Lee et al [10] studied the aeroelastic responses of the wind turbines and found that the turbulence generated by the upstream wind turbine had a significant impact on the fatigue load of the downstream wind turbine by simulating two 5MW wind turbines. Feng et al [11] quantified gearbox load spectrum variation and cumulative fatigue damage to predict gearbox service life by introducing different turbulence scales. Mou et al [12] showed that the optimal active yaw angle through the algorithm could effectively reduce the fatigue load of the blade. Taking two NREL 5MW reference wind turbines as the research object, Daniel et al [13] showed that a certain degree of positive yaw would reduce the blade, tower, and shaft bending load. At the same time, it was pointed out that the accuracy of the simulation results needed to be improved by the improvement of the simulation model. By building a three-dimensional wind field with wake characteristics, Sun et al [14] realized the aerodynamic simulation of various inflow wind conditions and yaw offset conditions; and further pointed out the dominant factors of fatigue load of offshore wind turbines under this simulation condition. To measure a 2.3MW wind turbine under wake conditions, Asmuth et al [15] verified six different fidelity model frameworks, indicating that most models could capture the main characteristics of the wake inflow and the resulting force on the downstream wind turbine.

In summary, there are many studies about the influence of yaw on the blade root load of wind turbines. However, there is a lack of research and analysis of blade root loads in realistic greedy control conditions based on operation data from actual wind farms.

Greedy control is a dynamic process, continuously adapting to inflow conditions. Simulations are hence typically not stationary, making the quantification of load statistics challenging. For this reason, it is convenient to approximate the original transient simulation by a set of stationary simulations where each sample corresponds to one yaw angle configuration, together with a probability distribution of the configurations to reconstruct load statistics. After this, the blade root load variation law is obtained while wake steering control is compared with the actual situation of greedy control.

The structure of the article is as follows: Chapter 2 mainly introduces the wind farm simulation model setting, example setting, and load post-processing calculation formula; in

Author Accepted Manuscript version of the paper by Jie Yan et al.
in 12th International Conference on Renewable Power Generation - RPG (2023)
DOI: http://dx.doi.org/10.1049/icp.2023.2492

Chapter 3, the output loads for the three control strategies are post-processed, and the load changes under the three strategies are compared. Finally, Chapter 4 gives the conclusion of this paper.

2. Simulation and case setup

2.1 Simulation setup

The wind turbine model is selected from the NREL 5MW reference wind turbine, and the relevant parameters of the wind turbine are shown in Table 1. The layout of the wind farm is shown in Fig 1.

Table 1 Key parameters of wind turbine

Wind turbine parameters	Value
Hub height	90m
Rotor diameter	126m
Cut-in, rated speed	6.9rpm, 12.1rpm
Cut-in, rated, cut-out wind speed	3m/s, 11.4m/s, 25m/s

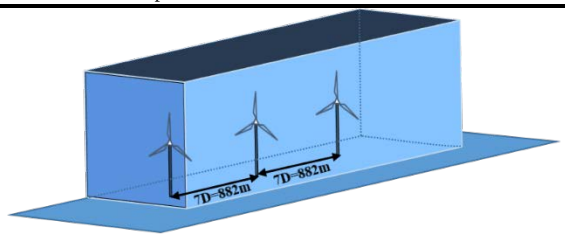

Fig. 1 Wind farm layout diagram.

Based on SCADA data from an offshore wind farm in the northeast of China, a representative hub height reference wind speed of 6.95 m / s has been identified, with a turbulence intensity of 10.32 %. This choice is based on the following: The hub height reference wind speed is the average of the selected-interval of operation time, and the turbulence intensity is the 90 % quantile over the interval. Turbulence boxes (ambient wind input files) using the standard IEC '-3' for offshore turbines with turbulence 10.32% is generated for the selected wind condition, using NREL's tool TurbSim.

In this paper, FAST.Farm is used to model the three wind turbines and the flow field in the wind farm, a configuration that has been successfully benchmarked to LES simulations [16]. Distinct turbulence boxes are used as input for the farm-level (low-resolution) and turbine-level (high-resolution) domains. The low-resolution covers the entire wind farm and plays a role in the wandering and merging of the wake. The time resolution of the low-resolution domain is 3s, the spacing of spatial nodes is set to 10.17m (horizontal transverse), 10m (horizontal longitudinal), 10m (height), the number of spatial nodes is 313 × 101 × 35, and the coverage of the wind farm is 3173m × 1000m × 340m. The high-resolution domain is developed around the wind turbine, which plays a role in the formation and inflow of the wake. The time step of the high-resolution domain is 0.1s, and the spacing of spatial nodes is set to be 10.17m (horizontal transverse), 10m (horizontal longitudinal), and 10m (height). The number of spatial nodes is 18 × 17 × 17, covering the range of 173m × 160m × 160m around the wind turbine, so as to carry out accurate aerodynamic load calculation.

The wake is fully developed after 200 s. The model in this paper outputs a load time series of 300 s-900 s for a total of 600 s, and the time step is 0.0125 s. The simulated output load includes the blade in-plane moment and the blade out-of-plane moment.

2.2 Yaw misalignment modelling

While active yaw control in wake steering can be straightforwardly modelled in the above-presented setup, changes in wind direction cannot. FAST.Farm relies on Tailor's frozen-turbulence assumption: changes in wind conditions are defined only at upwind boundary of the domain, then propagated (advected) downstream with the mean wind speed. This does not allow for modelling independent changes in wind direction for each turbine, as they will have to be correlated through a time shift. To circumvent this shortcoming, yaw misalignment is modelled by changing the yaw angle instead of wind direction. While this will yield the same apparent flow locally on the wind turbines, the effect on wake trajectory (meandering/deflection) and its relative position with respect to downstream turbines will be different. This source of uncertainty has been overlooked in this study and is left as further work.

2.3 Case setup

2.3.1 Test matrix: three control strategies are simulated, including the ideal situation of greedy control (GCI), the actual situation of greedy control (GCA), and wake steering control(WSC). GCI sets the yaw angle of 3 wind turbines to 0; GCA sets the yaw angles of the three wind turbines to 17.96, 16.81, and 0, respectively. These three yaw angles are the optimal yaw angles obtained by a wake steering algorithm based on the sequential least squares method (SLSQP) [17] under the current layout and wind conditions.

Based on the operating data of the above offshore wind farm, yaw misalignment statistic under the simulated wind condition are used to derive a probability distribution for the yaw angles to be used as proxy to changes in wind direction for GCA. This is shown in Fig 2. It is assumed that the probability distributions are equal and independent for the three turbines, consistently with the ergodic nature of turbulence; the effects of transients (e.g. gusts) and wakes are left as future work.

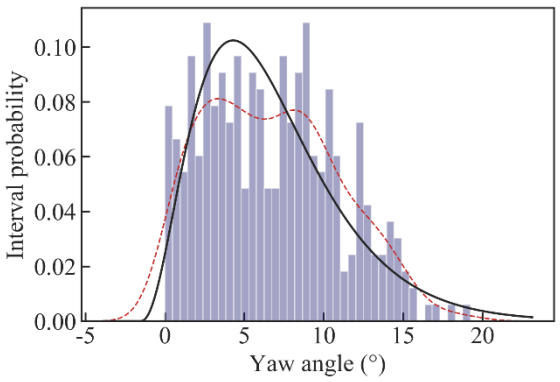

Author Accepted Manuscript version of the paper by Jie Yan et al.
in 12th International Conference on Renewable Power Generation - RPG (2023)
DOI: http://dx.doi.org/10.1049/icp.2023.2492

Fig.2 The probability distribution diagram of wind turbine's yaw angle based on SCADA data. The purple column is the probability of each based on the 40 bins; the red line is the density trend; the black line is the fitting probability trend

According to the 3σ rule, five yaw angle intervals are divided. The mean and probability of each interval are shown in Table 2.

Table 2 Statistical table of yaw angle under GCA

Yaw interval	Mean yaw angle	Interval probability
[0, 2.55)	1.28	0.186
[2.55, 6.73)	4.46	0.329
[6.73, 10.91)	8.74	0.317
[10.91, 15.09)	12.86	0.145
[15.09, 19.28)	16.6	0.023

Each wind turbine sets the average yaw angle of the above interval in turn, and the three wind turbines are carried out arrangement assemblage. A total of 125 cases were simulated under GCA.

2.3.2 Load post-processing: the maximum load and damage-equivalent load of the blade in-plane and out-of-plane moment are used to evaluate the load.

Define the maximum load as Equation 1, and the normalized maximum load as Equation 2 :

$$ML = max\left(max_{i=1}^{3}\left(load_{\mathrm{i}}(t)\right)\right) \quad (1)$$

$$ML_{norm} = \frac{ML}{ML_{standard}} \quad (2)$$

Among, *ML* is the maximum load; $load_i(t)$ is a load signal time series of the blade i; $ML_{norm}$is the normalized maximum load; $ML_{standard}$ is the maximum load normalization standard.

The damage-equivalent load is defined as Equation 3 and Equation 4, and the normalized damage-equivalent load is defined as Equation 5:

$$DEL_i = \left(\sum_{j=1}^{n}\frac{S_j^m}{N_{eq}}\right)^{\frac{1}{m}} \quad (3)$$

$$DEL = max_{i=1}^{3}(DEL_i) \quad (4)$$

$$DEL_{norm} = \frac{DEL}{DEL_{standard}} \quad (5)$$

In which DEL_i is the damage-equivalent load to the current load under study for blade i; S_j is the corresponding mean values of the load cycle j; N_{eq} is the reference number of cycles; the Whöler exponents (m) of the blades is 10. Since the wind turbine is three-bladed, the maximum value of the *DEL* over the three blades is taken as the effective *DEL*. DEL_{norm} is the normalized damage-equivalent load; $DEL_{standard}$ is the normalization standard.

2.3.3 Load expectation from the actual situation of greedy control: in order to represent continuous greedy control from GCA simulations, the loads obtained from the 125 combinations of yaw angles are assembled using the probability distribution in Table 2 to yield the actual situation of greedy control- equivalent load Leq, viz.

$$Leq(i_T, l) = \sum_{i=1}^{5} P_i\left[\sum_{j=1}^{5} P_j\left(\sum_{k=1}^{5} P_k \cdot L_{ijk}\left(i_T, l\right)\right)\right] \quad (6)$$

In which, *i, j, and k* represent the yaw angle of the three wind turbines respectively; P_i ,P_j, P_k are the assumed independent probabilities of the first, second and third wind turbines at five different yaw angles, respectively; L_{ijk} is the ML or DEL value of load type under study (represented by l) on wind turbine i_T for the yaw angle combination (*i, j, k*).

3 Results and analysis

In this chapter, firstly, according to the load time series obtained by simulating three strategies, the ML and DEL of the blade in-plane moment and the blade out-of-plane moment under the three strategies are calculated. Then, based on the load of the first wind turbine under GCI, normalization is carried out to explore the relative load change of each wind turbine under different strategies. This enables quantifying the effect on blade loads represented by WSC compared with GCA.

3.1 Maximum load

3.1.1 The blade in-plane moment: according to the equations in 2.3 and 2.4, the load time series obtained by simulating the three strategies are processed, and the ML values of the blade in-plane moment under the three strategies are calculated as shown in Table 3.

Table 3 The ML values of the blade in-plane moment under three strategies

The blade in-plane moment	GCI	GCA	WSC
Wind turbine_1_ML (kN·m)	4459.000	4383.215	4202.000
Wind turbine_2_ML (kN·m)	3971.000	3914.027	3925.000
Wind turbine_3_ML (kN·m)	3944.000	3894.591	4034.000

After normalization with the ML of the blade in-plane moment under GCI from the first wind turbine as the base, the variation trend of the ML values of the blade in-plane moment under three strategies is obtained as shown in Fig 3.

Author Accepted Manuscript version of the paper by Jie Yan et al.
in 12th International Conference on Renewable Power Generation - RPG (2023)
DOI: http://dx.doi.org/10.1049/icp.2023.2492

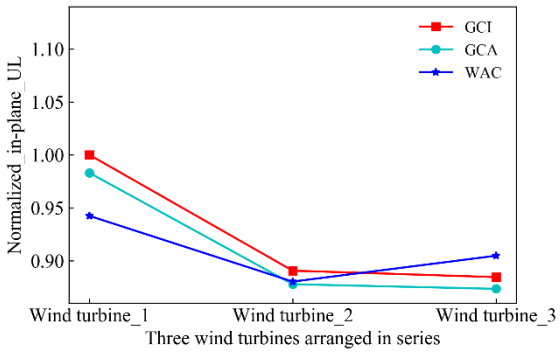

Fig. 3 Comparison of ML of normalized the blade in-plane moment under three strategies

From Fig 3, it can be seen that for the first wind turbine, the maximum ML value of the blade in-plane moment is GCI, and the minimum ML value of the blade in-plane moment is WSC. For the second wind turbine, the maximum ML value of the blade in-plane moment is GCI, and the minimum ML value of the blade in-plane moment is GCA. For the third wind turbine, the maximum ML value of the blade in-plane moment is WSC, and the minimum ML value of the blade in-plane moment is GCA.

The ratios between WSC and GCA are 95.87 %, 100.28 %, and 103.58 %, respectively.

3.1.2 The blade out-of-plane moment: similarly, the ML values of the blade out-of-plane moment under three strategies are calculated as shown in Table 4.

Table 4 The ML values of the blade out-of-plane moment under three strategies

The blade out-of-plane moment	GCI	GCA	WSC
Wind turbine_1_ML (kN·m)	7105.000	7091.195	6890.000
Wind turbine_2_ML (kN·m)	4874.000	4927.870	5364.000
Wind turbine_3_ML (kN·m)	4767.000	4848.628	5182.000

After normalization with the ML of the blade out-of-plane moment under GCI from the first wind turbine as the base, the variation trend of the ML values of the blade out-of-plane moment under three strategies is obtained as shown in Fig 4.

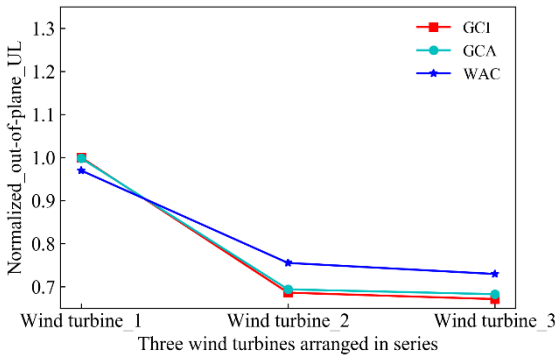

Fig. 4 Comparison of ML of normalized the blade out-of-plane moment under three strategies

From Fig 4, it can be seen that for the first wind turbine, the ML value of the blade out-of-plane moment is GCI, and the minimum ML value of the blade out-of-plane moment is WSC. For the second wind turbine, the maximum ML value of the blade out-of-plane moment is WSC, and the minimum ML value of the blade out-of-plane moment is GCI. For the third wind turbine, the maximum ML value of the blade out-of-plane moment is WSC, and the minimum ML value of the blade out-of-plane moment is GCI.

The ratios between WSC and GCA are 97.16 %, 108.85 %, and 106.88 %, respectively.

3.2 Damage-equivalent load

3.2.1 The blade in-plane moment: according to the equations in 2.3 and 2.4, the load time series obtained by simulating the three strategies are processed, and the DEL values of the blade in-plane moment under the three strategies are calculated in Table 5.

Table 5 The DEL values of the blade in-plane moment under three strategies

The blade in-plane moment	GCI	GCA	WSC
Wind turbine_1_DEL (kN·m)	5979.876	5909.776	5828.342
Wind turbine_2_DEL (kN·m)	5818.038	5725.273	5612.012
Wind turbine_3_DEL (kN·m)	5799.780	5708.085	5688.040

After normalization with the DEL of the blade in-plane moment under GCI from the first wind turbine as the base, the variation trend of the DEL values of the blade in-plane moment under three strategies is obtained as shown in Fig 5.

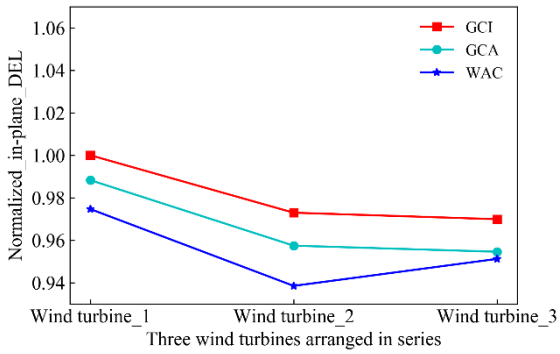

Fig. 5 Comparison of DEL of normalized the blade in-plane moment under three strategies

It can be seen from Fig 5 that the maximum DEL values of the blade in-plane moment from the three wind turbines are all GCI, and the minimum DEL values of the blade in-plane moment from the three wind turbines are all WSC.

The ratios between WSC and GCA are 98.62%, 98.02%, and 99.65%.

Author Accepted Manuscript version of the paper by Jie Yan et al.
in 12th International Conference on Renewable Power Generation - RPG (2023)
DOI: http://dx.doi.org/10.1049/icp.2023.2492

3.2.2 The blade out-of-plane moment: similarly, the DEL values of the blade out-of-plane moment under three strategies are calculated in Table 6.

Table 6 The DEL values of the blade out-of-plane moment under three strategies

The blade out-of-plane moment	GCI	GCA	WSC
Wind turbine_1_DEL (kN·m)	2163.510	2210.172	2244.759
Wind turbine_2_DEL (kN·m)	1671.582	1774.709	2218.157
Wind turbine_3_DEL (kN·m)	1738.469	1857.761	2044.295

After normalization with the DEL of the blade out-of-plane moment under GCI from the first wind turbine, the variation trend of the DEL values of the blade out-of-plane moment under three strategies is obtained as shown in Fig 6.

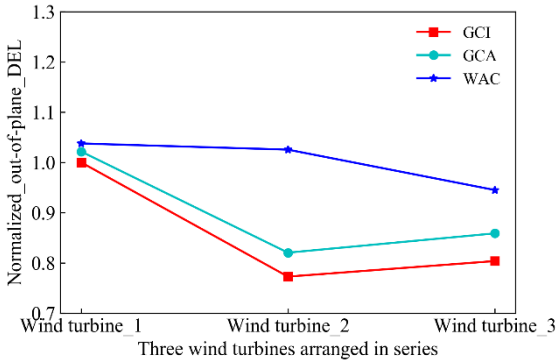

Fig. 6 Comparison of DEL of normalized the blade out-of-plane moment under three strategies

It can be seen from Fig 6 that the maximum DEL value of the blade out-of-plane moment from the three wind turbines is WSC and the minimum DEL value of the blade out-of-plane moment is GCI.

The ratios between WSC and GCA are 101.56%, 124.99%, and 110.04%.

4 Conclusion

In this paper, aiming at addressing the lack of research and analysis of the blade root load caused by wake steering control compared with naturally-happening yaw misalignment due to changes in wind direction, a probability distribution of yaw misalignment angles corresponding to a specific wind condition is derived from SCADA data from an actual offshore wind farm. This is used to model actual operation in standard greedy control, estimating load statistics (maximum and damage-equivalent) from stationary simulations through fixed yaw angles instead of time-varying wind direction. Results are compared against ideal (no yaw misalignment) and actual (misalignment from varying wind direction) greedy control operation. The conclusions are as follows: compared with actual greedy control, wake steering control reduces the maximum load of the blade in-plane and out-of-plane moment from the first wind turbine; the maximum load of the blade in-plane and out-of-plane moments from the other two wind turbines is increased. The damage-equivalent load of the blade in-plane moment from the three wind turbines is reduced. The damage-equivalent load of the blade out-of-plane from three wind turbines is increased. Further work will assess the effect of representing changes in wind direction as yaw angles (through wake trajectories), and introduce correlation in probability distributions for yaw misalignment.

5 Acknowledgements

This work was supported by the National Key Research and Development Program of China (No.2019YFE0104800), the Research Council of Norway through the CONWIND project (grant nr. 304229) and FME NorthWind research centre (grant nr. 321954).

6 References

[1] Li, L., Han, S., Wang, Y., et al.: 'Impact of atmospheric stability on wind turbine wake velocity distribution', International Conference on Renewable Power Generation, 2015, pp. 1-5.

[2] Munters, W., Meyers, J.: 'Optimal dynamic induction and yaw control of wind farms: effects of turbine spacing and layout', Journal of Physics: Conference Series. IOP Publishing, 2018, 1037, (3), pp. 032015.

[3] Fleming, P., King, J., Dykes, K., et al.: 'Initial results from a field campaign of wake steering applied at a commercial wind farm-Part 1', Wind Energy Science, 2019, 4, (2), pp. 273-85.

[4] Howland, M. F., Lele, S. K., Dabri, J.O., et al.: 'Wind farm power optimization through wake steering', Proceedings of the National Academy of Sciences, 2019, 116, (29), pp. 14495-14500.

[5] Zhao, L., Gong, F., Chen, S., et al.: ' Optimization study of control strategy for combined multi-wind turbines energy production and loads during wake effects', Energy Reports, 2022, 11, (8), pp. 1098–1107.

[6] Fleming, P., Gebraad, P., et al.: 'Evaluating techniques for redirecting turbine wakes using SOWFA', Renewable Energy, 2014, 70, pp. 211-218.

[7] Gomez-Iradi, S., Astrain, D., et al.: ' Numerical Validation of Wind Plant Control Strategies', Journal of Physics: Conference Series, 2020, 1618, (2), pp. 022010.

[8] Campagnolo, F., et al.: 'Wind tunnel testing of wake control strategies', Proceedings of the 2016 American Control Conference, 2016, pp. 513–518.

[9] Damiani, R., Dana, S., Annoni, J., et al.: 'Assessment of wind turbine component loads under yaw-offset conditions', Wind Energy Science, 2018, 3, (1), pp.173–189.

[10] Lee, S., Churchfield, M., Moriarty, P., et al.: 'A Numerical Study of Atmospheric and Wake Turbulence Impacts on Wind Turbine Fatigue Loadings', Journal of Solar Energy Engineering, 2013, 135,(3), pp. 031001.

[11] Feng, Y., Qiu, Y., Yang, W., et al.: 'Wind turbulence impacts to onshore and offshore wind turbines gearbox fatigue life', 3rd Renewable Power Generation Conference, 2014, pp. 1-5.

[12] Lin, M., Porté-Agel, F.: 'Power Maximization and Fatigue-Load Mitigation in a Wind-turbine Array by Active Yaw Control: an LES Study', Journal of Physics: Conference Series. IOP Publishing, 2020, 1618, (4), pp. 042036.

[13] Zalkind, D.S., Pao,L.Y.,: ' The fatigue loading effects of yaw control for wind plants,' Proceedings of 2016 American Control Conference, 2016, pp. 537–542.

[14] Sun, J., Chen, Z., Yu, H., et al.: 'Quantitative evaluation of yaw-misalignment and aerodynamic wake induced fatigue loads of offshore Wind turbine', Renewable Energy, 2022, 199, pp. 71-86.

[15] Asmuth, H., P. Navarro Diaz, G., et al. : 'Wind turbine response in waked inflow: A modelling benchmark against full-scale measurements', Renewable Energy, 2022, 191, pp. 868-887.

[16] Shaler, K., Jonkman, J.: 'FAST.Farm development and validation of structural load prediction against large eddy simulations', Wind Energy, 2021, 24, (5), pp. 428-449

[17] Luo, Y., He, Z., Che, X.: 'Hyperchaotic sequence least squares method for solving nonlinear equations and its application', Journal of Hunan University of Arts and Sciences: Natural Science Edition, 2010, 22(1), pp. 36-39